Contents lists available at ScienceDirect

# Nuclear Inst. and Methods in Physics Research, A

# The large COMPASS polarized solid ammonia target for Drell–Yan measurements with a pion beam

V. Andrieux [e], A. Berlin [a], N. Doshita [c,*], M. Finger [d], M. Finger Jr. [d], F. Gautheron [a,e], N. Horikawa [f], S. Ishimoto [g], T. Iwata [c], Y. Kisselev [h,1], J. Koivuniemi [a,e], K. Kondo [c], A. Magnon [l], G.K. Mallot [i], J. Matoušek [d], T. Matsuda [j], W. Meyer [a], Y. Miyachi [c], G. Nukazuka [c,2], M. Pešek [d], C. Pires [k], C. Quintans [k], G. Reicherz [a,*], St. Runkel [b], A. Srnka [m], H. Suzuki [f]

[a] *Ruhr-University Bochum, 44780 Bochum, Germany*
[b] *University Bonn, 53115 Bonn, Germany*
[c] *Yamagata University, Yamagata, 990-8560, Japan*
[d] *Charles University in Prague, 18000 Prague, Czech Republic*
[e] *University of Illinois at Urbana-Champaign, Urbana, IL 61801-3080, USA*
[f] *Chubu University, Kasugai, 487-8501, Japan*
[g] *KEK, Tsukuba, 305-0801, Japan*
[h] *JINR, 141980 Dubna, Russia*
[i] *CERN, 1211, Geneva 23, Switzerland*
[j] *University of Miyazaki, Miyazaki, 889-2192, Japan*
[k] *LIP, 1049-003 Lisbon, Portugal*
[l] *CEA-Saclay, DAPNIA, 91191 Gif-sur-Yvette, France*
[m] *Institute of Scientific Instruments, ASCR, 61264 Brno, Czech Republic*

## ARTICLE INFO

## ABSTRACT

The transversely polarized target (PT) of the COMPASS (NA58) collaboration at CERN has been used for Drell–Yan measurements in 2015 and 2018. The transverse spin structure of the proton has been studied using a negative pion beam and a solid ammonia target. Employing the dynamic nuclear polarization (DNP) method, proton polarization values of more than 80% have been routinely achieved after one day, at a homogeneous magnetic field of 2.5 T and using a $^3$He/$^4$He dilution refrigerator. During the data-taking the target operates in a transversely oriented magnetic dipole field at 0.6 T. This so-called frozen spin operation mode without the DNP pumping process leads to a slow depolarization of the target material, which is further accelerated by the heat input of the pion beam, produced secondary particles and radiation damage effects to the target material. Ammonia has the highest resistance against radiation-induced depolarization among known solid target materials. The proton polarization has been measured by the nuclear magnetic resonance (NMR). Relaxation times of about 1100 h have been observed for the proton polarization resulting in an average polarization between 68% and 76% during about two weeks long data-taking periods. To achieve a systematic uncertainty of the polarization $\Delta P/P$ as low as 3.2% and a statistical one of less than 1.8% two large target cells with appropriate positioning of the NMR-coils have been built.

## 1. Introduction

Since 2002 the COMPASS (Common Muon and Proton Apparatus for Structure and Spectroscopy) collaboration has focused on studies of the spin structure of the nucleon and hadron spectroscopy with high energy muon and hadron beams [1]. To study the transverse structure of the proton, measurements of a single polarized Drell–Yan

(DY) process with a $\pi^-$ beam and a transversely polarized proton target were proposed [2]. At leading twist and considering the transverse momentum of a parton, the structure of the proton can be described with eight Parton Distribution Functions (PDFs). Only three of them survive after integration over the transverse momentum of a parton $k_T$. The other five PDFs are called TMD (Transverse Momentum Dependent) PDFs. Sivers function $f_{1T}^\perp$ is one of the TMD PDFs and describes the

---

correlation between $k_T$ and the transverse component of the proton spin [3]. This function can be measured via DY and Semi-Inclusive Deep Inelastic Scattering (SIDIS). The sign of $f_{1T}^{\perp}$ measured via DY is predicted from theory to be reversed with respect to the one measured via SIDIS [4]. A confirmation of this prediction is a crucial test for the TMD approach in QCD and one of the main purposes of the polarized DY measurements at COMPASS.

The spin asymmetries in the angular distribution of a dimuon from the pion induced polarized DY process $\pi^- + p \rightarrow \mu^+ + \mu^- + X$ are measured. The $\pi^-$ beam with a momentum of 190 GeV/c is provided by the CERN-SPS. Given the small cross section of the DY process, to obtain reasonable statistics a beam intensity of about $10^8$ pions/s and a target with sufficient length along the beam direction had to be employed. In order to keep systematic effects under control, the polarized target system was required the capability to periodically rotate the proton spin in transverse directions. In addition, due to the pion beam – in contrary to earlier experiments with muon beams – radiation effects have to be considered not only for the particle detection and data acquisition systems, but also for the Polarized Target (PT) apparatus.

After describing the PT apparatus upgrade in Section 2, some changes in the experimental set-up due to the increased radiation exposure during the DY measurements are described in Section 3. In Section 4, the new design of the COMPASS target cells, made of polychlorotrifluoroethane (PCTFE) is presented. For the transversely polarized proton, ammonia as target material is used and its overall effective polarization degree is a key factor. The advantages of ammonia over other polarized proton target materials are reviewed in Section 5. The preparation and the activation of solid ammonia for the DNP are discussed in Section 6. In Section 7 the polarization measurements and interpolations over the various physics data periods are reported. Largest polarization values of +82.9% and −86.0% with an average accuracy of 3.2% for the systematic error and less than 1.8% for the statistical error were obtained. Taking into account the polarization losses due to the frozen spin operation mode, radiation and beam heating effects, an average proton polarization of about 70% in the whole target cells were obtained.

## 2. Polarized target apparatus

The PT apparatus in the initial layout of the COMPASS experiment is based on the system built for the SMC (NA47) experiment [5,6]. It is a composition of several systems with a high cooling power $^3$He/$^4$He dilution refrigerator, two superconducting magnets, microwave system, a target container with two separated target cells and multiple NMR detection system in order to monitor the proton polarization of $NH_3$.

As target material, ammonia ($NH_3$) is used. Especially its radiation hardness and the high dilution factor favor ammonia among others as a proton target for the DY measurements (see Section 5). To obtain a reasonable luminosity at a beam flux of about $10^8$ pions/s, the target has to be extraordinarily large. The target material of a volume of about 1380 cm$^3$ was filled into two cells. The double cell configuration is employed, i.e. the target material in the two cells is polarized in the opposite direction to each other to cancel the false asymmetry due to time-dependent effects originating from acceptance variations (beam and apparatus). In the experiment, the beam profile has an approximate Gaussian distribution and the $2\sigma$ of the profile is adjusted to $\pm 2$ cm. The stability of the beam center position for long term is less than 1 mm. The target cell diameter is chosen to be 40 mm, in order to reduce the multiple scattering of the produced particles in the target material itself, too. Each target cell has a cylindrical shape with a length of 550 mm and they are separated by a 200 mm gap, sufficient to identify from which target cell the events of interest originate. Ten continuous wave NMR circuits monitor the polarization at different points along the large target. The target cells are further discussed in Section 3.

At the beginning of COMPASS, the target magnet system of the SMC was still used, until it was upgraded in 2005. The opening angle of the superconducting magnet was increased from $\pm 69$ mrad to $\pm 180$ mrad. The large-acceptance magnet system consists of a solenoid and a dipole magnet providing a magnetic field of 2.5 T and 0.63 T, respectively. The solenoid magnet supplied the magnetic field for longitudinal[3] polarizations during the DNP. Several trim-coils along the solenoid are installed to ensure a field homogeneity $\Delta B/B$ of about 10 to 50 ppm in the target region over an approximate distance of 130 cm. The dipole magnet is used for transverse polarization and the rotation of the target spin. Once the material is polarized, the refrigerator is operated in the frozen spin mode.[4] In this mode, the direction of the target spin can be rotated with negligible losses of the polarization. The spin direction follows the superposition of both fields, either for the transverse mode or for a complete spin reversal. Usually, the latter procedure is done periodically to reduce systematic errors, but only during runs with longitudinal target polarizations[5] (see Section 7). In 2005 together with the magnet system the microwave cavity was renewed in order to match the improved opening angle and to fulfill the need of simultaneous DNP with opposite signs in the two separate target cells. The microwave cavity which is fed by two 70 GHz microwave sources (EIO[6] tubes) is separated into two halves with a microwave stopper between the up- and downstream cells,[7] to reduce the influence of the tuned microwaves at the neighbor cell. The microwave stopper between the cells is made from a combination of a carbon-honeycomb-grid, copper-foil and -mesh. Each EIO tube has an output power of 20 W, whereat only a few watts reach the entrance of the microwave cavity, in which the electron spins absorb a power of about 40 to 400 mW during the polarization build-up [7].

An ultra-low temperature system with high cooling power is essential to obtain a high nuclear polarization. The $^3$He/$^4$He-dilution refrigerator is able to maintain temperatures between 100 to 300 mK during the DNP and approximately 60 mK during the frozen spin mode within the data-taking period in spite of the additional heat load induced by the pion beam. In Fig. 1, the side view of the apparatus is shown. The COMPASS refrigerator is designed as a horizontal target, which is aligned with the particle beam. The target material can be accessed by removing the whole target holder unit, which fits exactly into the dilution refrigerator, joint with a tight indium seal. In order to minimize unwanted substances in the beam line, there are two 0.1 mm stainless steel windows and several aluminum foils in addition to the target material — for the beam entrance and thermal shielding, respectively. The mixing chamber is made of glass-fiber reinforced epoxy and has 70 mm in diameter and 0.6 mm wall thickness. At the bottom of the target cells, a CuNi pipe with holes is supplying uniformly $^3$He into the mixing chamber. The basic principle of a dilution refrigerator can be looked up in [8,9].

The $^3$He/$^4$He-circuit is connected to eight mechanical booster pumps in series, with a total pumping rate of 13,500 m$^3$/h, which removes the $^3$He from its diluted phase and feeds it back to the mixing chamber. A separate cooling circle (only $^4$He) supplies the superconducting magnets and serves as a heat exchanger for the incoming $^3$He liquefaction. Multiple temperature sensors are installed in the vicinity of the target material as well as at critical points along the cooling circuit. Most of the sensors are electronic elements, such as diodes and resistors, but there is also the option to measure the temperature by the helium vapor pressure. The pre-cooling period is mostly monitored by silicon diodes, whereas the ultra-low temperatures in the mixing chamber are best measured with ruthenium-oxide resistors (see Section 3).

---

[3] The terms longitudinal and transverse are used in relation to the beam direction.

[4] At ultra-low temperatures ($\approx 100$ mK) the nuclei have relaxation times of several thousand hours.

[5] Field rotation during transverse mode would cause more systematic errors due to changes of the beam path.

[6] EIO stands for Extended Interaction Oscillator.

[7] Upstream is the first cell facing the beam, whereas downstream has a contrary meaning.
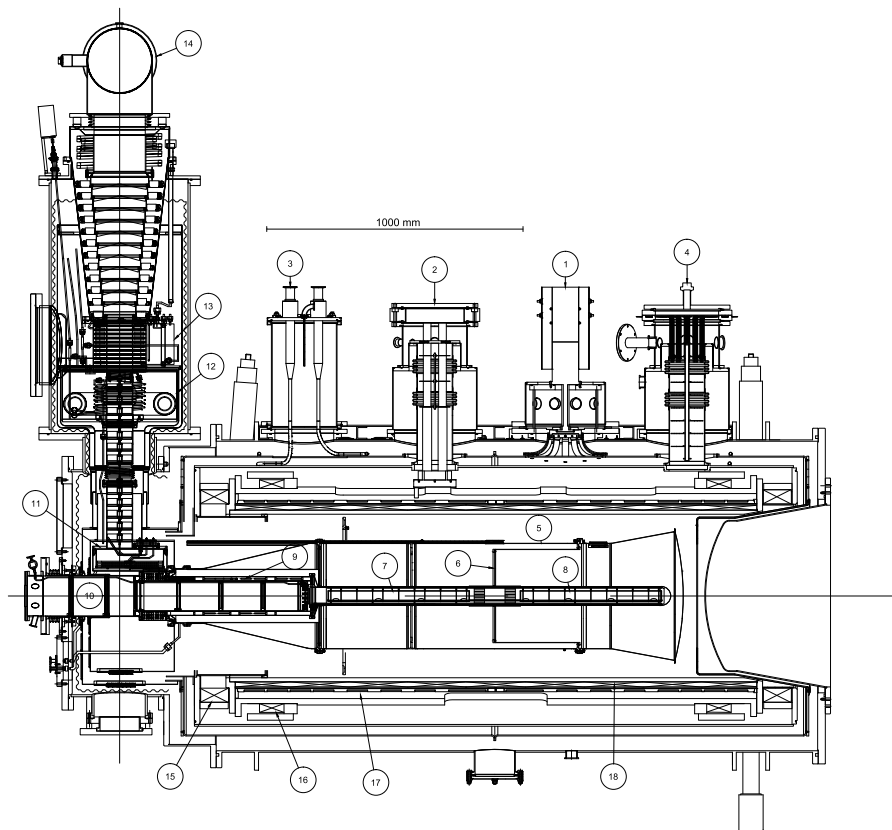
**Fig. 1.** Side view of the COMPASS polarized target in Drell–Yan physics data-taking 2015 and 2018: ① cryocooler for magnet thermal radiation shield, ② current lead turret, ③ liquid nitrogen precooling inlet and outlet connections, ④ liquid helium transfer and instrumentation turret, ⑤ microwave cavity, ⑥ microwave stopper, ⑦ upstream and ⑧ downstream target cell inside aramid–epoxy tube, ⑨ step heat exchanger, ⑩ target holder isolation vacuum and radiation shields, ⑪ still or helium-3 evaporator, ⑫ helium-4 evaporator, ⑬ helium-4 gas/liquid separator ⑭ helium-3 pumping port, ⑮ upstream end compensation coil, ⑯ dipole magnet, ⑰ trim coils and ⑱ solenoid magnet.

These resistors and also the method of using the vapor pressure for the temperature measurement are needed for the Thermal Equilibrium (TE) calibration, which is crucial to calculate the proton polarization (see Section 6). During the DNP, so-called speer resistors (carbon) are used to estimate the absorbed microwave power (bolometric) for each cell.

## 3. Radiation exposure during Drell–Yan measurements

The CERN Radiation Protection Committee set limitations for the operation with muon and hadron beams. Another restriction is set in the amount of material allowed along the beam line, by limiting the pion interaction length of material crossed. [2]. To fulfill the needs for the DY-measurements, several changes have to be made for both, the spectrometer and the target system. In Fig. 2 the absorber is pictured. It is placed between the target and the spectrometer to stop unwanted hadrons, whereas the muons are able to pass almost unhindered. This absorber is necessary to reduce the high secondary particle flux and thus prevents the tracking detector from data saturation. The absorber is 236 cm long and consists of aluminum-oxide followed by a steel body, encased in stainless steel frames and having a long core of tungsten in the center, for stopping the primary non-interacting beam [10]. The tungsten device has a length of 140 cm and its diameter varies from 85 cm to 95 cm (see Fig. 2). Due to the pion beam flux of about $10^8$ pions per second, further consequences are directly related to the polarized target, such as a local heating of the ammonia material by the beam as well as the total heat input in the dilution refrigerator. While the local heating can be controlled sufficiently by the beam focus and the chip size of the target material, a total heat input of 5 to 9 mW must be cooled away at beam rates of $6 \times 10^7$ pions/s to $10^8$ pions/s, respectively [7]. In order to ensure a sufficient cooling, the flow rate

must be raised, which leads to higher temperature within the mixing chamber. In addition, the radiation damage caused by the pion beam to the ammonia material has to be considered. All these effects have a negative influence, whether on the maximum target polarization or the polarization loss rate.

Another issue is the radiation exposure of the target containments, which are directly hit by the beam. FLUKA simulations[8] for the estimation of the radiation exposure during the DY-measurement were made [11]. In Fig. 3 a close view of the accumulated dose for the target is shown. During 180 days of data acquisition, a flux of $10^8$ pions/s and a beam spot size with $\sigma \leq 1$ cm is assumed. Also significant positions of the target are indicated in the plotted simulation result. Noticeable is, that the highest radiation dose appears very downstream of the target, due to the secondary produced particles along the target. A maximum dose of 16 kGy/year reaches at a radius of 2 cm around the beam, whereas in the center the dose may reach 40 kGy/year.

On the target cell surface at r = 2 cm, several temperature sensors are mounted and they are exposed to the high radiation as well. An investigation of the radiation hardness of new materials for the target container and the sensors was done in collaboration with a group at the Jülich proton cyclotron and at ELSA (Electron Stretcher Accelerator) in Bonn, as shortly mentioned in the next section.

In order to prevent the high radiation level around the target apparatus during the DY data-taking, the magnet control system was placed outside the experimental area, where the radiation dose was about 10 uSv/h. In addition, the magnet cryogenics control CPU was shielded by concrete blocks, polyethylene and boron-carbide to protect it from neutrons. The control room was moved to another building 700 m

---

[8] FLUKA (FLUktuierende KAskade) – a Monte Carlo simulation software for interactions of particles in matter.
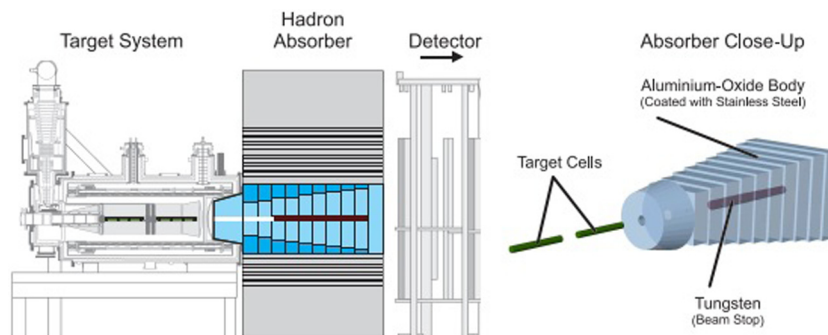
**Fig. 2.** Hadron absorber for the DY-measurements. The left figure shows the position of the absorber with respect to the polarized target apparatus and the spectrometer. The right figure shows the main part of the absorber layout with the beam-stop plug and the aluminum-oxide body, together with the respective position of the target cells.
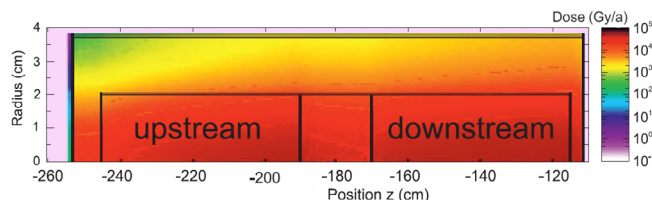


**Fig. 3.** Accumulated dose in Gray per year. Target center is located at $Z = -180$ cm.
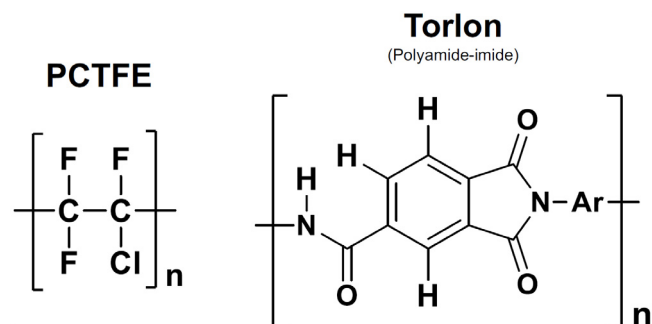


**Fig. 4.** The chemical structure of PCTFE and Torlon.

away from the experimental hall. Over 250 PT-related parameters are monitored by the Detector Control System (DCS) developed on SIMATIC WinCC.[9]

## 4. New target container for Drell–Yan measurements

The container should safely contain the target material. However, it may become as highly stressed as the material itself (see Fig. 3) due to the radiation with the pion beam. So far, the container was made of a polyamide net, reinforced by a glue Stycast. The advantage of such a net is of course the small amount of matter, which may less interfere with scattered particles, but the drawbacks, in addition to the uncertainty in the radiation resistance, are contaminations with hydrogen. Both, the net and the Stycast-glue contain hydrogen, which contributes to the hydrogen resonance signal of ammonia, since some of the NMR coils are mounted onto the surface of the container.

To verify the integrity at high radiation dose, three different materials, namely FEP (Fluorinated Ethylene Propylene), PCTFE and Torlon (trademark name of Polyamide-imides) were exposed to ionizing radiation. All three materials were irradiated at ELSA with an electron beam up to 40 kGy. Additionally, PCTFE and all other different materials
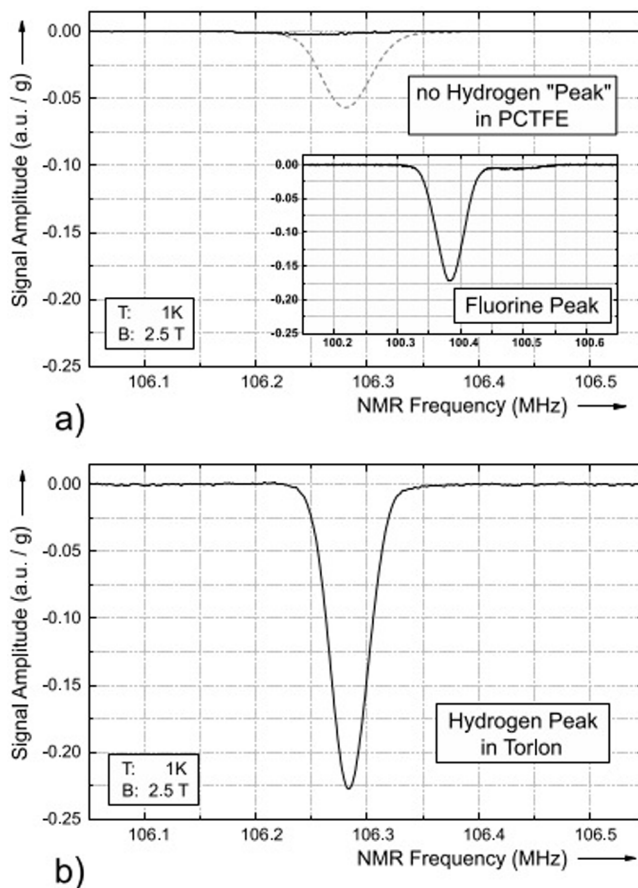
**Fig. 5.** Measurement of the TE signals of Fluorine in PCTFE and hydrogen in Torlon (see text).

of the previous target cells were tested with a proton beam at the proton cyclotron in Jülich. Of course, the external conditions of the COMPASS experiment could not be reproduced. In Bonn, the samples were kept in liquid argon (87 K) during the irradiation, whereas in Jülich, the materials were at room temperature and irradiated under atmospheric conditions. The dose rates went up to 2.5 Gy/s and the total dose of 20 kGy was applied within 5 h, instead of the expected dose for a complete experimental year at COMPASS. Therefore, these tests can only be used as reference points for the characteristics in the DY experiment. The detailed results are discussed in Ref. [12]. FEP and Torlon were excluded as materials for the target cells, because FEP has a smaller tensile strength compared to PCTFE and Torlon contains hydrogen. The structural formula of PCTFE shows no hydrogen (Fig. 4).
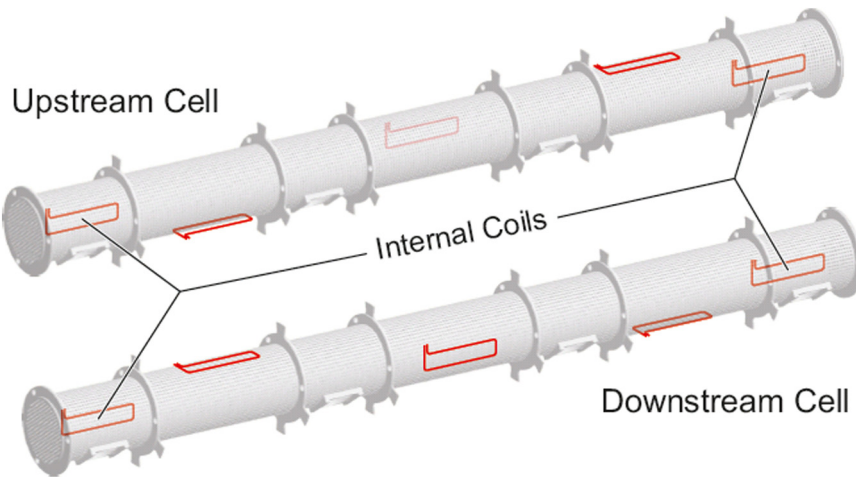
**Fig. 6.** The target cells configuration in 2015 [12]. NMR coils are drawn with red lines. Three and two coils are placed outside and inside each cell, respectively.
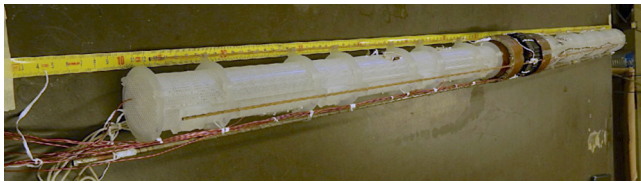


**Fig. 7.** Target cell photo with NMR coils.

Experimentally this fact was confirmed by measurements at the Bochum University. The results are shown in Fig. 5. In the graph of PCTFE, the TE-signal $^{19}$F is displayed in the inset. No signal was measured for hydrogen in PCTFE, as shown by the prospect of the contamination of one hydrogen atom per repeating unit (dashed line). In Torlon, the TE-signal of hydrogen is clearly visible, which confirms the expectation of its structural formula. Besides the hydrogen in Torlon, a group at the Jefferson Laboratory has revealed that the hydrogen can be polarized dynamically, after the material is exposed to radiation [13]. This behavior would cause further uncertainty in the polarization measurement at the DY measurements at CERN.

After the thermal shrinkage of PCTFE ($\approx 0.91\,\%$) was measured and stress tests with several cool-down and warming-up cycles have shown a very good rigidity of PCTFE, newly designed PCTFE target cells have been built. The new target cell was designed in a modular system (see Fig. 6), which allows an easy replacement of defective sections, or even a rearrangement of the cell compartments. Besides the PCTFE bodies, the final cells set-up also includes microwave stopper, fixation rods, NMR coils and temperature sensors, as shown in Fig. 7. More technical details can be found in Ref. [12].

## 5. Ammonia as solid target material

Already in the 1960s, ammonia ($NH_3$) has been proposed as an attractive candidate for a polarized solid target material [14]. Its main advantage is a large fraction of polarizable nucleons $f$ (dilution factor) with respect to the total amount of nucleons per molecule. The dilution factor $f = 3/(14 + 3) = 0.176$ is the highest among the polarized solid targets for protons. At that time, the best results were obtained in ammonia doped with an ethanediol–Cr(V) complex. However, the 70% polarization [15,16] was not confirmed by later work at CERN [17] and ammonia was not introduced as a polarized target material. About ten years later in 1979 a maximum polarization as high as 90% was achieved at CERN when the necessary radicals for the DNP process were successfully produced by radiation for the first time [18]. This

triggered new activities in irradiation techniques. First hints of an improved polarization resistance against radiation damage (radiation hardness) compared to previously used alcohol target materials were reported in 1980 [19]. Altogether, these discoveries have been the motivation to continue experiments (EMC, SMC) with polarized muons and polarized proton targets at CERN. Although the radiation hardness of ammonia was not an issue for experiments with muons, this property makes ammonia an unrivaled candidate for the DY-measurements with pion beam. The importance of a high effective nucleon polarization $P_{eff} = P_t \times f$ of the molecule may be seen from the so-called target Figure Of Merit (FOM) in a particle physics experiment:

$$\text{FOM} = P_t^2 \times f^2 \times \rho \times \kappa \tag{1}$$

Due to the quadratic contribution, the dilution factor and the target polarization $P_t$ have the largest impact on the FOM and therefore, the quality and economical efficiency of the scattering experiment. The typical filling factor $\kappa$ of about 0.55 is linked to the shape of the material. Especially in experiments with a high intensity hadron beam, the dumped heat must be removed quickly, such that a loss of the nuclear polarization can be prevented [20].

The density $\rho$ (0.853 g/cm$^3$) is fixed through the choice of the material. The simpleminded dilution factor 3/17 of $NH_3$ depends on the target composition as well as on the physics process of interest: $f = \frac{n_H \sigma_{\pi^- H}^{DY}}{n_H \sigma_{\pi^- H}^{DY} + \Sigma_A n_A \sigma_{\pi^- A}^{DY}}$, where $n_H$ and $n_A$ represent the amount of polarizable protons and nuclei in the target respectively, and $\sigma^{DY}$ corresponds to pion-induced DY cross-section. The latter quantity was computed at NLO with a parton-level Monte-Carlo program [21], adapted to the case of a pion beam. The dilution factor is evaluated on a multi-dimensional grid covering the kinematic dependence of the DY cross-section. In the region of interest, the dilution factor is about 7% higher compared to the naive calculation and varies within 20% depending on the kinematics.

The COMPASS spectrometer cannot distinguish the scattering off protons between hydrogen and nitrogen. In ammonia, nitrogen $^{14}$N is also polarized. Due to the large quadrupole moment of $^{14}$N (spin 1 particle), its NMR-resonance signal has such a large spread that it cannot be recorded by a single frequency sweep. Systematic studies in ammonia have shown, that the nitrogen polarization can be calculated with the knowledge of the hydrogen polarization via equal spin temperature theory [22]. The correction due to the nitrogen polarization is in the order of 2% [23]. However, the maximum target polarization $P_t$ and the filling factor $\kappa$ depend on the target material production and its preparation. These procedures are discussed in the next section.
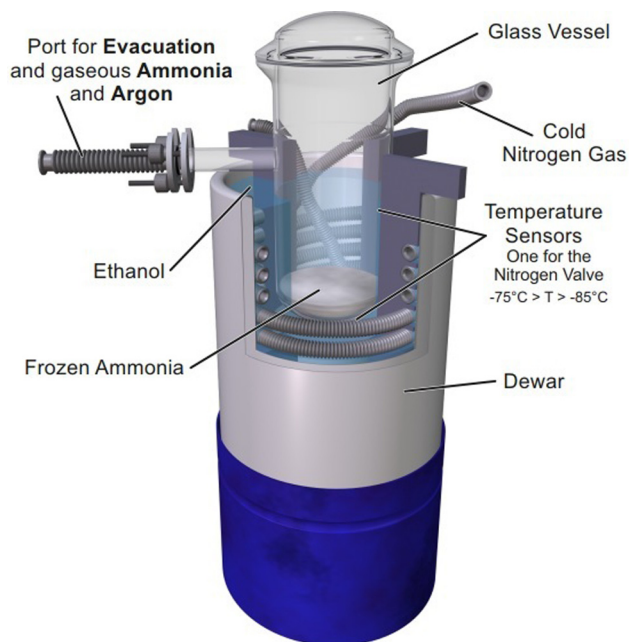
**Fig. 8.** Illustration of the solidification device for ammonia.



**Fig. 9.** Illustration of the irradiation refrigerator.

## 6. Preparation and DNP-activation of solid ammonia

In order to use $NH_3$ for the COMPASS experiment, the particular challenge was the development of a mass production technique, which ensured the preparation of about 0.75 kg (about 1.5 liters) of highly polarizable granules of this material. The usual and well-established way to produce an alcohol target like butanol, is adding a chemical radical in form of a powder and dropping the mixture into a bath of liquid nitrogen. As a result, small glassy spheres of 1 to 2 mm in diameter can be produced in a reliable way on a large scale. However, ammonia is a gas at room temperature. Liquefying in the first place and dropping liquid ammonia into a liquid nitrogen bath was attempted [24,25], but as a result, the ammonia spheres were very fragile and had gas pockets in it, which led to a non-uniformity of the material and even destruction during irradiation [26,27]. The solution was to freeze liquid ammonia slowly under controlled conditions below 195.4 K to a transparent solid with a crystalline structure [28]. Afterwards, the solid block was crushed into small pieces and the shredded material was sieved in order to select the small fragments with a final size of 2 to 3 mm. A picture of the new designed device for the solidification process is shown in Fig. 8.

With this apparatus the average amount of solid ammonia produced is around 30 g per day. Details of the entire solid ammonia production process are described in Ref. [12].

The next step is the creation of the paramagnetic centers, i.e. of unpaired electrons. In order to allow the DNP mechanism to operate, a suitable amount ($10^{-4}$ to $10^{-3}$ per nucleus) of paramagnetic centers has to be implanted into the material. For this purpose the granules were exposed to the 20 MeV electron beam of the Bonn injection LINAC in batches of 150 to 170 $cm^3$, each for about 10 h. During the irradiation, in which each sample received $10^{17}$ $e^-/cm^2$, the material was kept at a temperature of 87 K in liquid argon.[10] Not only working with strict safety regulations, but also special equipments are required. The irradiation refrigerator is illustrated in Fig. 9, whereas details are given in [12].
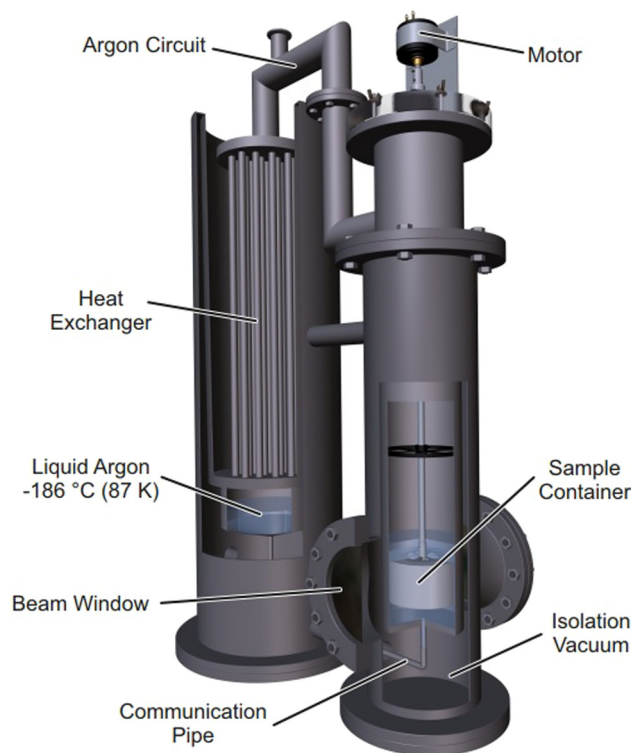
A conspicuous sign for the irradiation is a color change of ammonia into an intense purple, see the picture in Fig. 10. This color can be used to evaluate the uniformity of the irradiation, but it is not a guarantee for the ability of dynamic polarization. In fact, these point defects, so called F-centers[11] in the crystal structure of ammonia are not the only ones. The irradiation with high-energy electrons can be seen as a result of classical collisions between the incoming electrons and the resting lattice. The collision process can be pictured in the following reaction:

$$e^- + NH_3 \rightarrow \dot{N}H_2 + \dot{H} + e^- \tag{2}$$

For irradiated ammonia, electron paramagnetic resonance (EPR) studies have shown that the $\dot{N}H_2$ radical represents the dominant paramagnetic center, which is used for the DNP process. A look at the EPR-spectrum of irradiated ammonia reveals the resonance of the unpaired electron in the ammonia radical $\dot{N}H_2$, coupled to nitrogen and forms, all in all, nine possible transitions [30]. The resonance peaks are so closed together, that they cannot be resolved. The specific shape of the $\dot{N}H_2$ resonance (Fig. 11) is mostly caused by the crystalline structure of solid ammonia and depends on the orientation of the crystal within the magnetic field.

The satellite peaks next to the $\dot{N}H_2$ resonance are caused by atomic hydrogen, which is still trapped in the ammonia matrix. However, the strong hyperfine interaction of the electrons with the hydrogen nuclei (protons) result in a large shift of its g-factor, so that their Larmor-frequencies do not match any more with the usually applied microwave frequency. Therefore, the $\dot{H}$ radicals do not contribute to the enhancement of the DNP. But this does not mean that the atomic hydrogen and other defects may have no effect on the polarization at all. They may take part in the relaxation process and as a result, they could reduce the achievable maximum polarization. In general, the radical density is a parameter which has to be optimized. Here a

---

[10] As experiences have shown, irradiation in liquid nitrogen as coolant in open vessels have led to destructive explosions. These explosions are caused by very rapid decomposition of ozone, formed of oxygen, which are dissolved in liquid nitrogen Gregory and Nuttall [29].

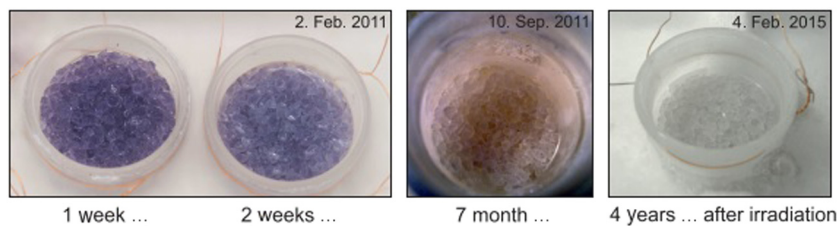[11] From the German word Farb-Zentrum, meaning color center.

**Fig. 10.** Color decay of irradiated ammonia. (For interpretation of the references to color in this figure legend, the reader is referred to the web version of this article.)
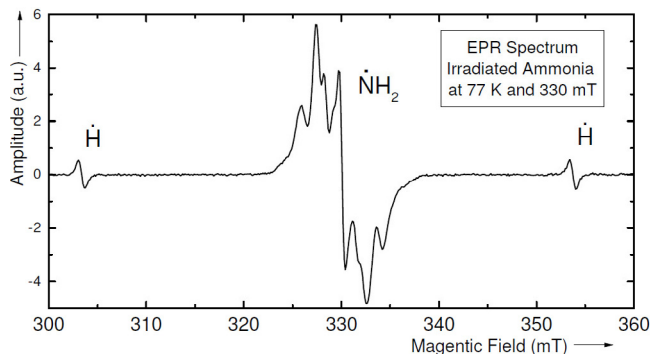


**Fig. 11.** EPR line of $\dot{N}H_2$.



**Fig. 12.** Absolute radical concentration versus time after irradiation for the fresh material in 2011.

compromise between build-up time and maximum polarization has to be found, since the radicals act also as relaxation channels.

For all irradiation batches prepared in 2011, the radical density of randomly chosen ammonia crystals was measured with a conventional X-band EPR spectrometer operating at 9.35 GHz. In order to prevent the paramagnetic centers from decaying, these studies as well as the storage of the ammonia material required the use of low (e.g. liquid nitrogen) temperatures. With the radiation mentioned above the average radical density was measured to be

$$C_{NH_3} = (4.24 \pm 0.2) \times 10^{19} \text{ spins/g.} \tag{3}$$

In the course of about 4 years after the material preparation by irradiation at the Bonn LINAC in 2011, detailed relaxation and polarization behavior studies of ammonia were performed in the Bochum laboratory. The results as well as a comparison to previously used material at COMPASS, which was produced in 1995, are documented in Ref [12]. A short summary is as follows: Two of the paramagnetic centers, namely the $\dot{N}H_2$- and $\dot{H}$ radical, are both active in the relaxation process, but only the $\dot{N}H_2$ radical is used in the DNP process. The purple color of ammonia started to fade out after a few weeks, which can be seen in Fig. 10.

After almost a year, the ammonia has lost its color completely and appears as transparent as before the irradiation. Nonetheless, the ability for DNP still remains, just like the material, prepared 1995, impressively demonstrated. Still changes in the polarization behavior were observed, namely on the relaxation time and the radical concentration, e.g. a reduction of the absolute radical concentration by about a factor of two in the first year after the radiation Fig. 12.

For the operation mentioned above, ammonia samples should be handled at temperatures below 100 K. At a temperature of 115 K, the F-centers are lost, which can be seen by a sudden disappearance of these centers, i.e. the purple color [26]. Important is the stability of the $\dot{N}H_2$-radicals, which are responsible for the DNP process. Detailed EPR-studies have been performed in the Bochum polarized target laboratory with an up-graded EPR apparatus, starting to work from 4 K to room temperature. Measurements have shown that a remarkable decay of the $\dot{N}H_2$-radicals starts at 100 K, whereas at 130 K the EPR resonance signal was not detectable already after a couple of minutes [31].
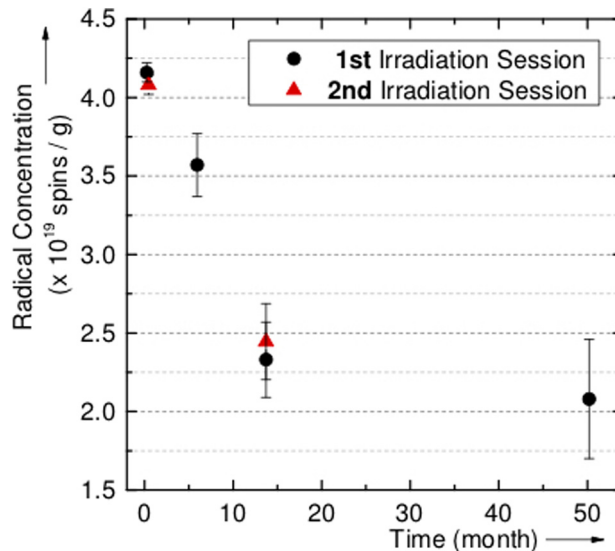
## 7. Polarization measurement

The proton polarization was measured with the well established NMR method. A diagram of the NMR system is illustrated in Fig. 13.

Five NMR coils were installed in each target cell. The coils were made of a stainless steel wire and were wound in a rectangular shape with a dimension of 50 mm × 10 mm. Three coils were fixed on the surface of the cell, while two coils were wrapped with a PCTFE foil of 50 μm thickness and placed inside the cell. Especially these inner coils, buried in the target material, were sensitive to heat and radiation induced effects along the beam spot path. A so-called Liverpool Q-meter [32] for phase sensitive detection of the NMR signals was connected to each NMR coil, forming a series LRC circuit tuned to 106.4 MHz, which is the proton Larmor frequency at 2.5 T.

The calibration of the proton polarization in $NH_3$ is based on the TE method, in which the respective NMR signals at the nominal field of 2.5 T are taken in the evaporative $^4$He-mode of the refrigerator at temperatures of 1.0, 1.3 and 1.5 K. In Fig. 14 a characteristic proton signal obtained under these conditions is shown, which corresponds to a polarization of about 0.25%. On the other hand the thermal equilibrium polarization $P_{TE}$ can be calculated by means of the Brillouin function $B_I$

$$P_{TE} = B_I(\mu B / k_B T) \tag{4}$$

which – at given temperature T and magnetic field $B$ – only depends on the spin quantum number $I$ and the magnetic moment $\mu$ of the respective nucleus. Since the nuclear polarization is proportional to the integrated intensity of the NMR spectra, the enhanced nuclear polarization $P_{dyn}$ is then determined by comparing the integrated signal
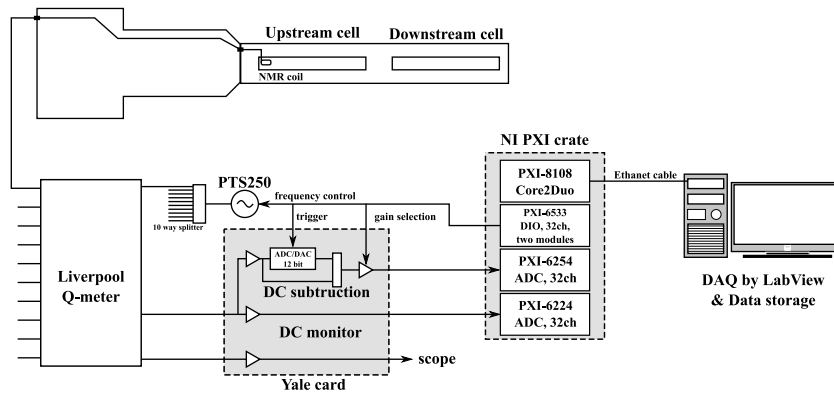
**Fig. 13.** A diagram of the polarization measurement system. Only one NMR coil is drawn.
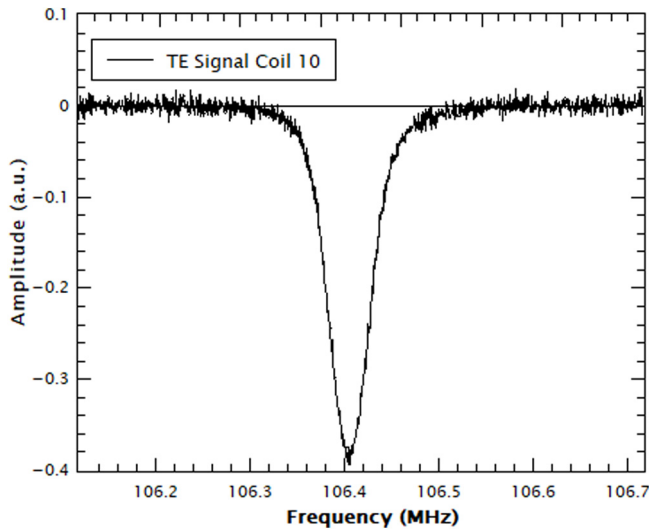


**Fig. 14.** A typical TE signal of coil no. 10 at $T = 1$ K is shown.



**Fig. 15.** The polarization of the each target cell as a function of time in 2015 and in 2018. Black (Red) points indicate the average polarization of the five coils in the upstream (downstream) cell. (For interpretation of the references to color in this figure legend, the reader is referred to the web version of this article.)

(area under the line shape) $A_{dyn}$ to that of the TE signals $A_{TE}$ according to the formula:

$$P_{dyn} = \frac{A_{dyn}}{A_{TE}} P_{TE}, \qquad (5)$$

where $\frac{A_{dyn}}{A_{TE}}$ is the calibration constant, listed in Table 1. As can be seen from formula (4), the polarization measurement depends on a precise knowledge of both, magnetic field and temperature. The magnetic field is well known by the frequency measurement of the NMR signals. The temperature during the TE calibration was measured by the helium vapor pressure and ruthenium-oxide (RuO) resistors. The radiation hardness of the RuO-resistors was checked up to 20 kGy with no change in their reproducibility [12]. Due to the PCTFE material of the target cell, the proton contribution from other materials than $NH_3$ – assumed to be water ice during the tricky loading process of the refrigerator – was about 5% compared to about 30% in previous COMPASS experiments. Once this contribution to the TE measurement is determined – by a so-called empty target measurement with the unloaded $NH_3$ at the end of the experiment data-taking – the calibration constant of each NMR coil is fixed. Relative statistical errors of the polarization of the ten NMR coils varied between 0.2 to 1.8% (see Table 1). The sources of systematic uncertainty in the polarization measurement are summarized in Table 2.

The circuit nonlinearity was estimated from the modulation depth. The sensitivity, depending on the Q-meter frequency, reflects the influence due to the drift of the Q-meter and tuned resonance circuit components. The phase error has an impact on both the TE signals and the
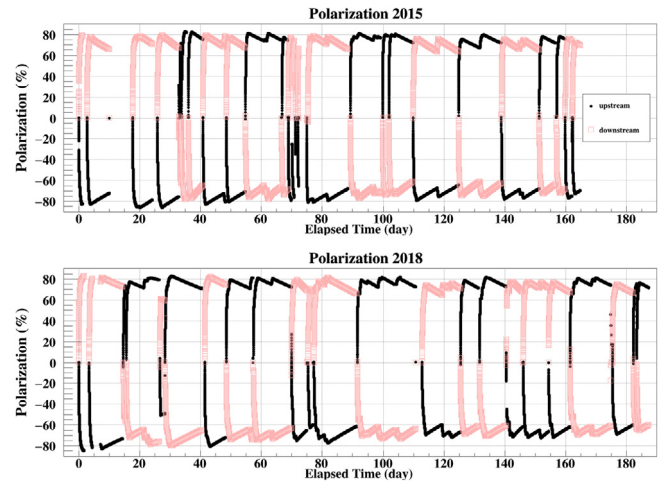
**Table 1**
Calibration constants and their relative statistical errors obtained from the TE calibration in 2015 and in 2018.

| | 2015 | | 2018 | |
|---|---|---|---|---|
| Coil # | Calibration constant | Statistical error (%) | Calibration constant | Statistical error (%) |
| 1 | −38.13 | 0.52 | −55.38 | 0.41 |
| 2 | −17.71 | 1.70 | −21.40 | 0.90 |
| 3 | −27.36 | 0.47 | −47.26 | 0.33 |
| 4 | −21.33 | 1.14 | −23.73 | 1.79 |
| 5 | −33.40 | 0.22 | −43.10 | 0.39 |
| 6 | −15.06 | 1.20 | −13.39 | 0.98 |
| 7 | −9.00 | 1.77 | −18.63 | 1.18 |
| 8 | −17.55 | 0.36 | −33.67 | 0.43 |
| 9 | −14.70 | 0.58 | −13.91 | 1.26 |
| 10 | −36.22 | 0.37 | −42.25 | 0.57 |

enhanced signals by the DNP. Low Frequency (LF) gain variation comes from the error in the gain measurement of the so-called Yale-cards. The total relative systematic error for the polarization measurement is estimated to be 3.2%.

For the process of the dynamical polarization the refrigerator is operated in the $^3$He/$^4$He dilution mode at temperatures around 100 to 350 mK depending on the actual microwave power.

The physics data-taking consisted of a series of a data-taking period of two weeks. Each data-taking period was divided into 2 sub-periods with opposite orientation of the polarization in the two target cells. At
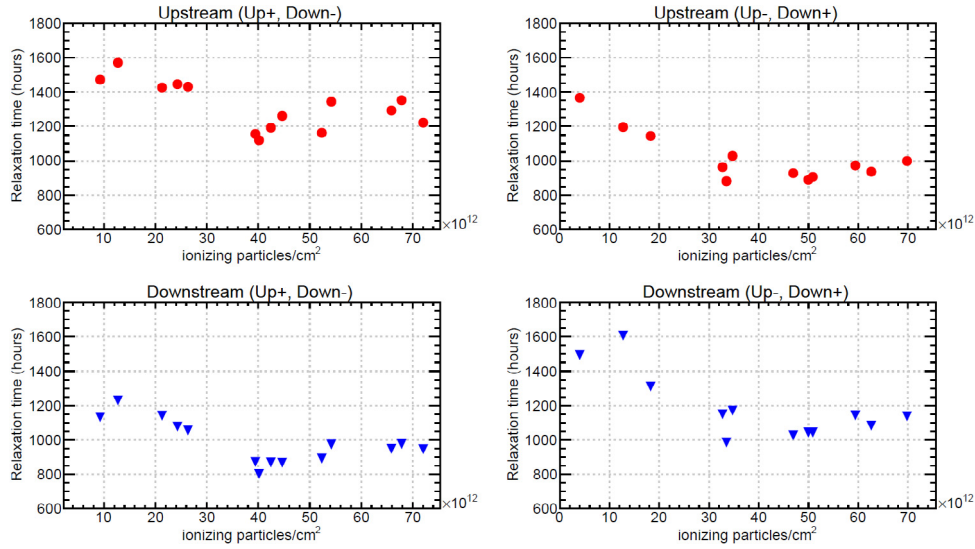
**Fig. 16.** Proton relaxation time (hours) as a function of ionizing particles per cm$^2$ in 2018. Upper left: Positive polarization in upstream cell. Upper right: Negative polarization in upstream cell. Lower left: Negative polarization in downstream cell. Lower right: Positive polarization in downstream cell.

**Table 2**

Relative systematic error estimated for the polarization measurement.

| Source of systematic uncertainty | $\Delta P/P$ (%) |
|---|---|
| Circuit non-linearity | 0.7 |
| Q-meter frequency dependent sensitivity for TE | 0.2 |
| and for enhanced signal | 0.2 |
| Baseline fitting | 0.2 |
| Fitting for TE signal | 1.0 |
| LF gain variation | 0.05 |
| Temperature measurement | 0.8 |
| Total | 3.2 |

**Table 3**

The maximum polarizations and the average polarizations over the physics data-taking in 2015 and 2018.

| Year | Cell | Maximum polarization (%) | Average polarization over the physics data-taking (%) |
|---|---|---|---|
| 2015 | Upstream | 82.7–86.0 | 74.2–71.4 |
| | Downstream | 79.3–77.8 | 69.2–67.0 |
| 2018 | Upstream | 82.9–84.7 | 76.3–68.3 |
| | Downstream | 82.0–80.0 | 73.6–68.5 |

**Table 4**

Average relaxation times of upstream or downstream cell in 2015 and in 2018.

| Year | Cell | Beam | Positive polarization (h) | Negative polarization (h) |
|---|---|---|---|---|
| 2015 | Upstream | On | 1400 | 1200 |
| | | Off | 3600 | 2900 |
| 2015 | Downstream | On | 1000 | 740 |
| | | Off | 4900 | 1700 |
| 2018 | Upstream | On | 1300 | 1000 |
| | | Off | 2500 | 1200 |
| 2018 | Downstream | On | 1100 | 1000 |
| | | Off | 1600 | 2100 |

the beginning of the first sub-period, the proton polarization was built up for about 24 h at 2.5 T in the longitudinal direction with respect to the beam and reached about 80%. Subsequently, the target was cooled down to about 60 mK to operate the polarized target in the frozen spin mode. This ensured a long polarization relaxation time even at 0.63 T dipole magnetic field. By an interplay with the solenoid and dipole magnetic fields the target spin was rotated into the needed transverse direction with respect to the pion beam. During the rotation process a polarization loss of 1% was observed.

After sub-periods of physics data-taking, the spin was rotated to the 2.5 T longitudinal field to measure the remaining polarization. To minimize systematic errors, the second sub-period followed by changing the microwave frequencies, polarize the protons in the two target cells in the opposite spin configuration compared to the first sub-period and rotate the spin subsequently in the opposite transverse direction for data-taking.

The proton polarization was not measured during the physics data-taking at the 0.6 T transverse dipole field, as the NMR system was optimized for measurements in the 2.5 T longitudinal solenoid field. Polarization values during the physics data-taking were interpolated by $P_t(t) = P_0 exp(-t/\tau) + P_{TE}$, where $\tau$ characterizes the rate of polarization loss (relaxation time) during the time interval t, started with the initial polarization $P_0$. The history of the average polarization values of each target cell for the runs in 2015 and in 2018 is shown in Fig. 15.

Routinely about 80% proton polarization after one day of DNP build-up were measured as summarized in Table 3 along with the average polarization during the physics data-taking time. The relaxation time depended on the target cell, the sign of the polarization and the beam condition as summarized in Table 4.

Obviously, the relaxation times without the beam were longer compared to those with the beam. In addition, beam heating effects were

more serious in the downstream cell due to an increased target temperature of 5 mK compared to the upstream cell. The average relaxation time during the data-taking period as a function of the ionizing particles per cm$^2$ is plotted in Fig. 16.

A simulation for secondary produced particles per incoming pion beam particle has given a factor of five. The total accumulated number of particles were about $0.7 \times 10^{14}$ per cm$^2$ in run 2018. For ionizing particles of more than $10^{13}$/cm$^2$ a reduction of the maximum proton polarization of $NH_3$ was already measured with an 2 GeV electron beam [33]. A global look on the average relaxation times (see Table 4) shows a stronger reduction of the negative polarization values compared to the positive ones in the frozen spin mode at 0.6 T.

Polarization time measurements in absence of the holding field – ramping down the magnetic field from 2.5 T to zero and after 5 min back to 2.5 T – may be a hint for this behavior: $\tau = 11$ minutes for positive polarization and $\tau = 7.5$ minutes for negative polarization values.

## 8. Conclusion

The COMPASS PT system successfully performed its operation with the target material $NH_3$ for Drell–Yan measurements with a pion beam. In order to provide the needed large amount of this material, reliable improved techniques for its production and irradiation have been developed. By means of systematic EPR studies it could be shown that for irradiated ammonia the $\dot{N}H_2$ -radical represents the dominant paramagnetic center, which is used for the DNP process. The optimum concentration of these centers was measured to be $(4.24 \pm 0.2) \times 10^{19}$ spins/g. Maximum proton polarization values of +82.9% and −86.0% were achieved at a magnetic field of 2.5 T within one day by means of DNP. During the data-taking the target operated at a transversely oriented magnetic dipole field at 0.6 T. This field value has required the frozen spin operation mode of the refrigerator without DNP pumping. As a consequence various depolarization effects, such as heat input and radiation damage effects produced by the pion beam, have led to a depolarization of the ammonia target material. Average proton polarization values between 68% and 76% have been determined by the nuclear magnetic resonance (NMR) method for the various physics data-taking periods. Relative statistical polarization errors from the measurements in the ten NMR coils varied between 0.2% and 1.8% in the two large volume target cells, built from the proton free material PCTFE. The relative systematic error is estimated to be 3.2%. All together, ammonia has demonstrated its superior figure of merit as polarized solid target material during the pion beam induced Drell–Yan experiments at CERN.

## CRediT authorship contribution statement

**V. Andrieux:** Resources. **A. Berlin:** Resources. **N. Doshita:** Writing – review & editing. **M. Finger:** Resources. **M. Finger Jr.:** Resources. **F. Gautheron:** Resources. **N. Horikawa:** Resources. **S. Ishimoto:** Resources. **T. Iwata:** Resources. **J. Koivuniemi:** Resources. **K. Kondo:** Resources. **A. Magnon:** Resources. **J. Matoušek:** Resources. **T. Matsuda:** Resources. **W. Meyer:** Writing – review & editing. **Y. Miyachi:** Resources. **G. Nukazuka:** Resources. **M. Pešek:** Resources. **C. Pires:** Resources. **C. Quintans:** Resources. **G. Reicherz:** Writing – review & editing. **St. Runkel:** Resources. **H. Suzuki:** Resources.

## Declaration of competing interest

The authors declare that they have no known competing financial interests or personal relationships that could have appeared to influence the work reported in this paper.

## Acknowledgments

## References

[1] COMPASS Proposal, CERN/SPSLC 96-14, SPSLC/P297, 1996.
[2] COMPASS-II Proposal, CERN/SPSC-2010-014/P340, 2010.
[3] D. Sivers, Phys. Rev. D 41 (1990) 83.
[4] J.C. Collins, Phys. Lett. B 536 (2002) 43.
[5] J. Kyynäräinen, Nucl. Instrum. Methods A 356 (1995) 47.
[6] D. Adams, et al., Nucl. Instrum. Methods A 437 (1999) 23.
[7] N. Doshita, et al., Nucl. Instrum. Methods A 526 (2004) 138.
[8] W.J. Huiskamp, O.V. Lounasmaa, Rep. Progr. Phys. 36 (1973) 423.
[9] T. Niinikoski, The Physics of Polarized Targets, Cambridge University Press, 2020.
[10] M. Alexeev, Nucl. Phys. B 245 (2013) 263–266.
[11] A. Maggiora, M. Gianmaria, R. Longo, et al., Tech. Rep. COMPASS note 2013-10, CERN, 2013.
[12] A. Berlin, Polarized Solid Ammonia Targets for the COMPASS Experiment at CERN (Doctorial thesis), RU-Bochum, 2015.
[13] D. Crabb, D.B. Day, Nucl. Instrum. Methods A 356 (1995) 9.
[14] M. Borghini, Choice of Substances for Polarized Proton Targets, CERN, Nucl. Phys. Div., 66-3, 1966.
[15] K. Scheffler, Nucl. Instrum. Methods 82 (1970) 205.
[16] K. Scheffler, in: G. Shapiro (Ed.), Proc. 2nd Int. Conf. on Polarized Targets, LBL 500, UC 34 Physics, Berkeley, 1971, p. 271.
[17] T. Niinikoski, private communications.
[18] T. Niinikoski, J.M. Rieubland, Phys. Lett. 72 A (2) (1979) 141.
[19] U. Härtel, et al., in: C. Joseph, J. Soffer (Eds.), Proc. Int. Symp. High Energy Physics with Polarized Beams and Targets, Basel Birkhäuser, 1981, p. 449.
[20] P. Cameron, D. Crabb, A. Lin, et al., in: W. Meyer (Ed.), Proc. 4th Int. Workshop on Polarized Target Materials and Techniques, 1984, p. 143.
[21] R. Boughezal, J.M. Campbell, R.K. Ellis, et al., Color-singlet production at NNLO in MCFM, Eur. Phys. J. C 77 (2017) 7.
[22] Ch. Dulya, PHD Thesis, LA, UNIVERSITY OF CALIFORNIA, 1996.
[23] O.A. Rondon, Phys. Rev. C 60, 035201.
[24] W. Meyer, ISSN-0172-8733, Bonn University, 1982.
[25] S. Brown, et al., in: W. Meyer (Ed.), Proc. 4th Int. Workshop on Polarized Target Materials and Techniques, 1984, p. 66.
[26] T. Niinikoski, in: C. Joseph, J. Soffer (Eds.), Proc. Int. Symp. High Energy Physics with Polarized Beams and Targets, Basel Birkhäuser, 1981, p. 191.
[27] D. Crabb, private communication.
[28] R. Dostert, et al., in: W. Meyer (Ed.), Proc. 4th Int. Workshop on Polarized Target Materials and Techniques, 1984, p. 13.
[29] C. Gregory, C. Nuttall, COMPASS Collaboration, Tech. Rep. CERN AT/95-06, CERN, 1995.
[30] W. Meyer, et al., Nucl. Instrum. Methods A 215 (1983) 65.
[31] D. Buschert, Diploma thesis, RU-Bochum, 2005.
[32] G.R. Court, et al., Nucl. Instrum. Methods A 324 (1993) 443.
[33] K.H. Althoff, et al., in: W. Meyer (Ed.), Proc. 4th Int. Workshop on Polarized Target Materials and Techniques, 1984, p. 174.